Atomistic Features of the Amorphous-Crystal Interface in Silicon

ATOMISTIC FEATURES OF THE AMORPHOUS-CRYSTAL INTERFACE IN SILICON

Noam Bernstein, Michael J. Aziz, Efthimios Kaxiras
Division of Engineering and Applied Sciences, Harvard University, Cambridge, MA 02138

(Received ..... ; Accepted in final form .....)

Abstract.
We simulate the amorphous-crystal interface in silicon using a combination of interatomic potential molecular-dynamics and tight-binding conjugate-gradient relaxation. The samples we create have high quality crystalline and amorphous portions. We develop some localized measures of order to characterize the interface, including a missing neighbor vector and the bond angle deviation. We find that the measures of order interpolate smoothly from a bulk crystal value to a bulk amorphous value across a 7Å thick interface region. The interface structures exhibit a number of interesting features. The crystal planes near the interface are nearly perfect, with a few dimer defects similar to the Si(100) 2×1 reconstruction. Interfaces produced with one constant temperature simulation method are rough, with several layers of atoms forming $\langle 110 \rangle$ chains and (111) facets. A different simulation method produces more planar interfaces with only a few $\langle 110 \rangle$ chains.

1. Introduction

Silicon, often considered the prototypical covalent semiconductor, has been extensively studied both for its inherent scientific interest and because it is the basis for a wide range of technologies. Silicon based electronic devices typically use the crystalline diamond structure phase, but the amorphous phase is also quite important both as an intermediate stage in the processing of electronic devices and as the final state in photovoltaic devices. The process by which the amorphous phase becomes crystalline by propagation of the interface, which is referred to as solid phase epitaxial growth (SPEG), has been the subject of many experiments. It is a thermally activated process with an activation energy of 2.7 eV over ten orders of magnitude in interface speed, strongly indicating a unique growth mechanism [1, 2]. The activation strain and effects of interface orientation and doping have also been studied experimentally. Despite all this evidence the microscopic atomic mechanism responsible for SPEG is still unclear. Reliable simulations of this process, with their ability to provide perfect atomic resolution, could shed light on the microscopic details of crystallization. The first step towards such an understanding of SPEG is the creation and char-

acterization of realistic atomistic models of the amorphous-crystalline interface.

2. Methods

In our simulations of the crystal-amorphous interface we use the Stillinger-Weber empirical interatomic potential [3] and a tight-binding Hamiltonian [4] which gives a quantum mechanical treatment of bonding in the system. This tight-binding model was optimized to reproduce the energetics of low energy bulk structures of silicon, as well as point defects and activated states. These geometries were chosen as representative of the types of configurations expected in the amorphous and crystalline systems, including strained bonds, over and under-coordinated atoms, and activated states where bonds are being broken and reformed.

We created several samples by simulating a rapid melting and quenching experiment using the empirical potential. Using a constant temperature, constant stress molecular dynamics algorithm we melt 192 atoms (12 atomic layers) out of 256 atoms in a $[220] \times [2\bar{2}0] \times [004]$ supercell, or out of 320 atoms in a $[220] \times [2\bar{2}0] \times [005]$ supercell, keeping the remaining 64 atoms (4 atomic layers) or 128 atoms (8 atomic layers) at 100 K. For the samples corresponding to the smaller supercell, we keep the temperature constant by picking a small fraction of the atoms at each time step and randomizing their velocities with a Boltzmann distribution (stochastic velocity rescaling). For the samples corresponding to the larger supercell, we divide the sample into 5.43Å slabs parallel to the interfaces, and every 500 time steps we rescale all of the velocities in each slab to obtain the appropriate temperature (periodic velocity rescaling). We rapidly quench the molten portion with the modification of the bond angle forces suggested by Luedtke and Landman [5] to ensure that the quenched part of the system enters the amorphous phase, and then anneal the amorphous portion at 1000 K. This process creates a sample with some crystal and some amorphous atoms separated by two (001) interfaces due to the periodic boundary conditions. We then relax the resulting samples using our tight-binding Hamiltonian and a conjugate-gradient energy minimization algorithm. During this relaxation atoms move as much as half a bond length, and many bonds are broken and formed.

3. Structural Properties

To characterize the samples we study properties of the two adjacent bulk phases, such as the pair correlation and bond angle distribution

Table I. Coordination statistics for the crystalline and amorphous portions averaged over all samples of teach type.

Neighbor Num.	2	3	4	5
stochastic velocity rescaling samples				
crystal	0.0%	0.2%	99.5%	0.2%
amorphous	0.7%	2.9%	92.0%	4.4%
periodic velocity rescaling samples				
crystal	0.1%	0.4%	98.6%	0.9%
amorphous	0.1%	2.1%	94.5%	3.3%

functions. The pair correlation function shows the expected features, including sharp peaks at all ranges in the crystalline regions, and a sharp first neighbor peak but much broader second and fourth neighbor peaks in the amorphous regions. The bond angle distribution functions show peaks around the ideal tetrahedral angle of 109.5°, with RMS deviations of 7° and 13° for the crystal and amorphous regions, respectively. The coordination statistics, counting as a neighbor every atom within the first peak in the pair correlation function, 2.7 Å, are listed in Table I. The samples produced with periodic velocity rescaling have a substantially larger number of 4-fold coordinated atoms than the samples produced with stochastic velocity rescaling. In both types of samples most of the defects are over-coordinated atoms.

We also define two localized measures of order which allow us to study the interface with atomic resolution. The first is the sum of the nearest neighbor vectors of each atom $\vec{v_t}$, which gives a measure of the symmetry of the local environment around each atom. The second is the deviation of the bond angles around each atom from the ideal tetrahedral angle. This gives a localized measure of the bond bending. These quantities are approximately constant in the centers of the amorphous and crystalline phases and interpolate smoothly in the intermediate regions, as a function of the coordinate perpendicular to the interface. The width of these interface regions is about 7 – 8Å. A more detailed discussion of these results will be published elsewhere [9].

4. Atomistic Features

4.1. Plan-Views

In Fig. 1 we show plan-views of slabs parallel to the interface in order to demonstrate some of the atomistic features of the interface. Pan-

el (a) is a picture of an interface from one of the samples prepared by stochastic velocity rescaling. The atoms that were kept cold (colored green in the figure), are arranged into almost perfect alternating up and down chains aligned along $\langle 110 \rangle$ directions. In two instances there are defects in the crystal layer where atoms in adjacent chains come together to form dimers. One such defect can be seen at the top center of the picture in Fig. 1(a). These are quite similar to dimers seen in the 2×1 reconstruction of the Si(100) free surface, except that in these dimers all atoms are four-fold coordinated, with some bonds to atoms on the amorphous side of the interface that are not in crystalline positions. Some of the nominally amorphous atoms, those in the region that was melted and quenched (colored red in the figure), have actually been incorporated into the crystal lattice during the quench. This can be seen clearly in the vertical chain of red atoms along the right edge of the figure. The remaining amorphous atoms are more disordered although they retain the continuous random network structure. Fig 1(b) is a picture of an interface from a sample prepared by periodic velocity rescaling. The same types of features seen in the interfaces of samples prepared by stochastic velocity rescaling are also present here. There are three dimers, including one in the center left and two in the horizontal chain of crystal atoms near the bottom of the figure. There is also a prominent horizontal row of crystallized but nominally amorphous atoms, between the top two horizontal rows of crystal atoms.

In some of the samples prepared by stochastic velocity rescaling almost all of the nominally amorphous atoms visible in the plan-view are in crystal lattice positions. One example is pictured in Fig. 1(c). All of the red atoms within the slice pictured are either arranged in $\langle 110 \rangle$ chains, or belong to dimers between those chains. The constant temperature algorithm used can not maintain arbitrarily high thermal gradients, and the heat flow into the cold crystal atoms during the quench was fast enough to crystallize some of the liquid atoms before they were configurationally frozen in the amorphous phase.

4.2. Crystal Regions

It is apparent from the plan-views that the amorphous-crystal interfaces are not entirely planar. Some atoms exist in crystal like surroundings in the region that was melted and quenched. To analyze the true shape of the interface we can plot the crystalline atom positions, but this requires a localized definition of the crystal. We define as "crystalline" every atom which is bonded to two other crystal atoms that should be sharing a common neighbor. Using a visualization program to display

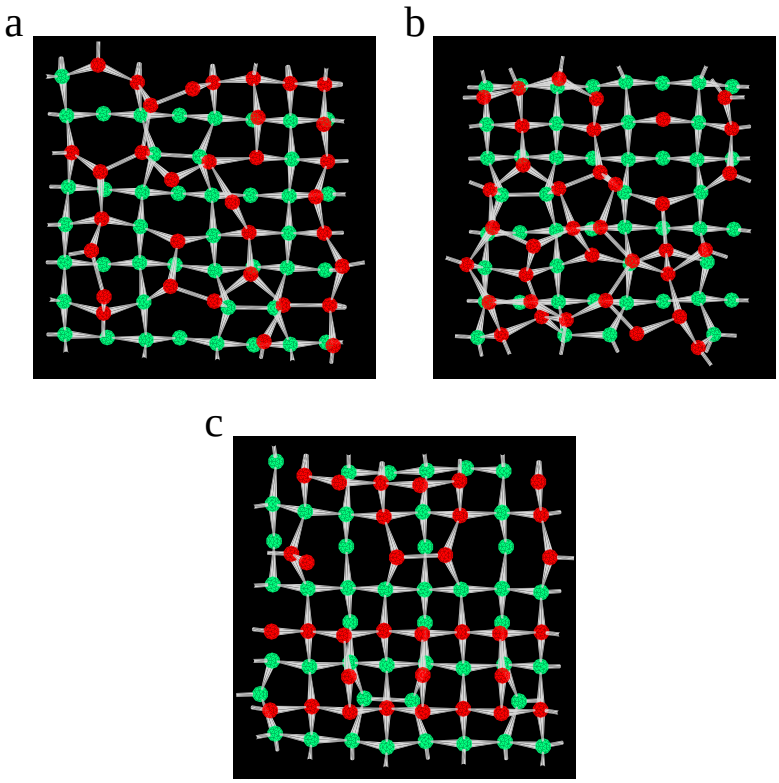

Figure 1. Plan-views of one interface from two samples prepared by stochastic velocity rescaling (a,c) and one interface from a sample prepared by periodic velocity rescaling (b). Atoms that were kept cold are in green and atoms that were melted and quenched are in red. The thick end of each bond is pointed out of the plane, the thin end into the plane, and cylindrical bonds are approximately parallel to the plane.

atomic configurations we manually examine each sample and select the atoms that are crystalline according to this criterion.

In Fig. 2 we show several views of the crystalline portion of a representative sample prepared using stochastic velocity rescaling. The four crystal layers that were kept cold are clearly visible in the center of the slab. In this instance three or four layers of crystal have grown on top of the original crystal portion, probably during the quench. Some additional crystal atoms are incorporated as $\langle 110 \rangle$ chains, for example a vertical chain at the right edge of Fig 2(c). In some cases mounds with small (111) facets have formed. One such facet on the bottom interface is viewed edge-on in Fig 2(b). The dimers described in the previous section are also present in the additional crystal layers, for example at the left of the top interface in Fig. 2(b).

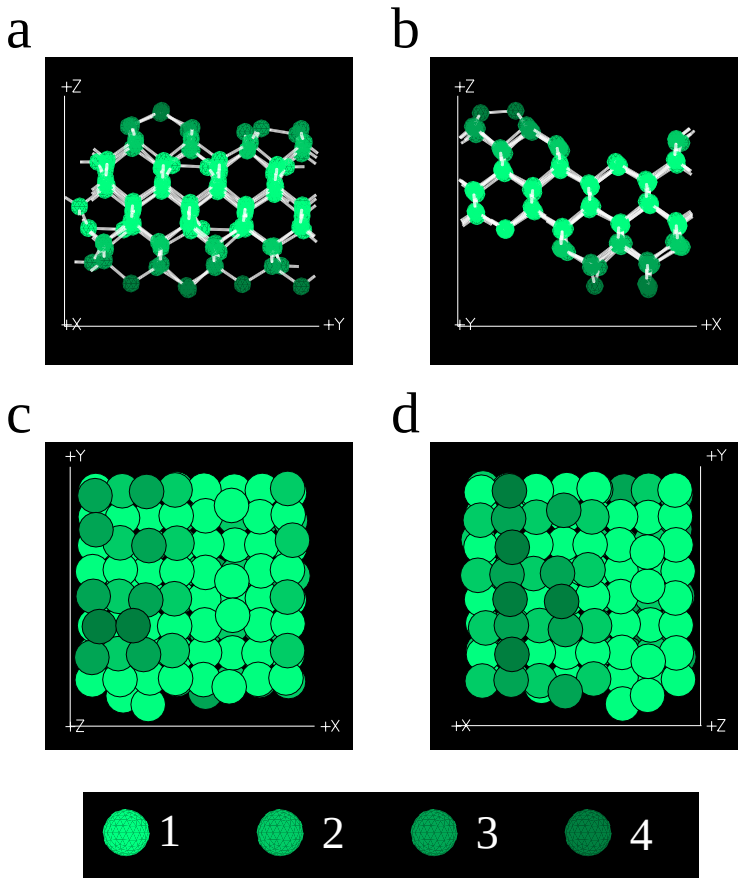

Figure 2. Views of crystal atoms of a representative sample prepared by stochastic velocity rescaling, along the x-axis (a), y-axis (b), z-axis from above (c), and z-axis from below (d). Atoms of type 1 are in the region that was kept cold throughout the simulation. Additional atoms (types 2–4) in crystal lattice positions (as described in the text) are also plotted, with darker colors as the distance from the interface plane increases.

In Fig 3 we show the corresponding views of the crystalline portion of a representative sample prepared using periodic velocity rescaling. The eight layers that were kept cold are visible at the center of the slab. There are several dimers present at the edge of this region, two at the top interface and three at the bottom interface in Fig 3(a). The interfaces are more planar than for the samples prepared with stochastic velocity rescaling, with only two or three additional layers of crystal, and no obvious (111) facets. Again, the additional crystal atoms are incorporated in $\langle 110 \rangle$ chains, such as the two vertical chains in Fig 3(c). Since there are no adjacent chains there are no dimers in

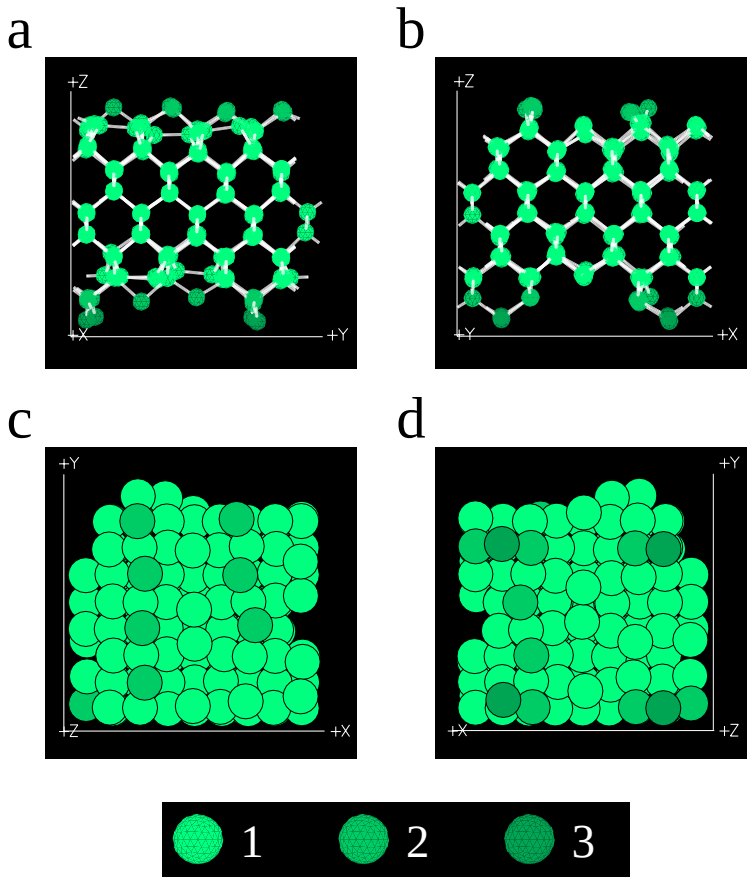

Figure 3. Views of crystal atoms of a representative sample prepared by periodic velocity rescaling, along the x-axis (a), y-axis (b), z-axis from above (c), and z-axis from below (d). Atoms of type one are in region that was kept cold throughout the simulation. Additional atoms (types 2 and 3) in crystal lattice positions (as described in the text) are also plotted, with darker colors as the distance from the interface plane increases.

the additional crystal layers. The qualitative differences between two types of samples are presumably caused by the different methods used for their preparation.

5. Conclusions

Using a combination of empirical interatomic potential molecular dynamics and tight-binding conjugate-gradient relaxation we simulated the amorphous-crystalline interface in silicon. The amorphous parts of the

samples show some order up to 7 Å and the characteristic lack of the third neighbor peak. Over 90% of the atoms in this region are four-fold coordinated, as would be expected for a good continuous random network model. Different methods for applying the constant temperature condition during the sample preparation can affect these values, although no qualitative differences were seen in samples prepared by two different approaches.

We computed two localized measures of order, the sum of the nearest neighbor vectors and the bond angle deviation around each atom. The behavior of these quantities as a function of the distance perpendicular to the interface plane reveals two approximately flat regions at the centers of the crystalline and amorphous phases, and a 7–8 Å thick transition region between the two. The interfaces exhibit a range of interesting features. The crystal atoms are ordered in $\langle 110 \rangle$ chains, with some defects resembling dimers on the free Si(100) surface. The atoms in the region that was melted and quenched are disordered, but some atoms near the interface have incorporated into crystal lattice positions. The atoms that have joined the crystal are arranged into $\langle 110 \rangle$ chains and (111) faceted mounds, creating rough interfaces, which are more prominent in the samples prepared with stochastic velocity rescaling. Samples prepared with periodic velocity rescaling exhibit more flat interfaces with only a few $\langle 110 \rangle$ chains.

References

1. G. L. Olson and J. A. Roth, Mater. Sci. Rep. **3**, 1 (1988).
2. G.-Q. Lu, E. Nygren, and M. J. Aziz, J. Appl. Phys. **70**, 5323 (1991).
3. F. H. Stillinger and T. A. Weber, Phys. Rev. B **31**, 5262 (1985).
4. N. Bernstein and E. Kaxiras, Phys. Rev. B **56** 10488, 1997.
5. W. D. Luedtke and U. Landman Phys. Rev. B **37**, 4656, (1988).
6. S. Kugler, G. Molnár, G. Petö, E. Zsoldos, L. Rosta, A. Menelle and R. Bellisent, Phys. Rev. B **40**, 8030 (1989).
7. I. Štich, R. Car, and M. Parrinello, Phys. Rev. B **44**, 11092 (1991).
8. Frans Spaepen, Acta Metallurgica **26**, 1167 (1978); F. Spaepen, in "Amorphous Materials, Modeling of Structures and Properties", edited by V. Vitek, TMS-AIME, New York (1983), p. 265.
9. N. Bernstein, M. J. Aziz, and E. Kaxiras, "The Amorphous-Crystal Interface in Silicon: a Tight-Binding Simulation," submitted for publication.

Address for correspondence: Noam Bernstein
522G McKay Lab
9 Oxford St.
Cambridge, MA 02138
phone: (617) 495-3392
FAX: (617) 496-4654
e-mail: noamb@cmt.harvard.edu